

### 3-D Finite Element Analysis Of Effect Cutting Edge Geometry on Cutting Forces ,Effective Stress , Temperature And Tool Wear In Turning

تأثير الشكل الهندسي لعدة قطع على قوى القطع , الاجهاد المؤثر , ودرجة الحرارة والبللى الحاصل في عملية الخراطة باستخدام تحليل العناصر المحددة ثلاثي الابعاد.

م.م.رحيم سعدون جميل  
الهندسة الميكانيكية /جامعة الكوفة

#### Abstract

The problem of tool wear monitoring in machining operations, has been an active area of research for quite a long time. The accurate prediction of tool wear is important to have a better product quality and dimensional accuracy. In cutting tools the area close to the tool tip is the most important region and conditions at the tool tip must be carefully examined, if improvements in tool performance are to be achieved

In this study, 3-D finite element modeling of precision hard turning has been used to investigate the effects of cutting edge micro-geometry on tool forces, temperatures , stresses and tool wear in machining of AISI 1045 steel using uncoated carbide inserts with four distinct edge preparations. Three type of edge preparation are redesign by using *software solid work 2008* , 1-honed edge(0.25 ,0.5 , 0.75 mm) , 2-chamfer (0.025 ,0,05 ,0.075 mm) , 3-land (15<sup>0</sup> and 0.05 ,0.1 ,0.2 ,0.3 mm) . Also perfectly sharp edge which is not prepared and redesign .

Simulation results for Hone micro-geometry inserts have tendency to result in lower forces, hence lower tool wear. Chamfer micro-geometry provides higher localized stress concentration. The highest stress and strain on workpiece occurred in the primary shear zone due to the highest deformation in this region, followed by the secondary shear zone. The maximum generated temperature was also found on secondary shearing zone .

#### الخلاصة :

أنجزت بحوث عديدة لفترات طويلة في ضبط او مراقبة مقدار البلى الحاصل في عدد القطع في عملية تشغيل المعادن.دقة تخمين البلى الحاصل في عدة قطع يلعب دور مهم في ضبط دقة الإبعاد و نوعية الإنتاج. في هذا البحث تم تطبيق العناصر المحددة (3D-FEA) في تشخيص تأثير الشكل الهندسي لأداة القطع على قوى القطع ,درجة الحرارة ,الاجهاد المؤثر والبلى الحاصل في عدة القطع أثناء تشغيل فولاذ AISI 1045 .تم إعادة تصميم وتهيئة ثلاث أنواع من حافات القطع وهي 1-حافة مدورة 2-حافة مشطوبة 3-حافة مائلة بزاوية وكذلك حافة باستخدام برنامج *Solid work 2008* . أظهرت النتائج بعد محاكاة هذه الأنواع باستخدام برنامج (Deform-3D) في حالة الحافة المدورة تميل إلى إنتاج قوى قطع قليلة وبلى قليل . إما في حالة الحافة المشطوبة تميل إلى توليد اجهادات عالية .الاجهادات والانفعالات العالية في المشغولة تكون في منطقة القص الأولية بسبب التشوهات العالية في هذه المنطقة تتبعها في المنطقة الثانوية .كذلك أظهرت النتائج إن أعلى درجات حرارة وجدت في منطقة القص الثانوية .

#### 1-Introduction

Hard turning is a popular manufacturing process in producing finished components that are typically machined from alloy steels with hardness between 50 and 70 HRc [1]. uncoated carbide cutting tools are widely used in hard turning. Uncoated carbide are designed with a certain micro edge geometry with a process called edge preparation. The effect of the edge preparation is to increase the strength of the cutting edge by providing a more gradual transition between the clearance edge and the rake face of the tool[2]. In order to improve the overall quality of the finished component, tool edge geometry should be carefully designed. Design of cutting edge may

affect the chip formation mechanism and therefore help to reduce cutting forces and increase tool life. It is known that sharp tools are not durable enough for most of the machining operations. Three common edge preparations are shown in figure 1 , are redesign by using software solid work 2008 , which are (a) honed edge ,(b) chamfer ,(c) land is  $15^{\circ}$  ,(d) perfectly sharp(no preparation).Combinations of these edge preparations are often applied to a single cutting edge to maximize the strengthening effect.

For the fifty years ago metal cutting researchers had developed many modeling techniques including analytical techniques, slip-line solutions, empirical approaches and finite element techniques In recent years, the finite element method has particularly become the main tool for simulating metal cutting processes[3].

There are numerous studies on 2-D FEA of orthogonal cutting which provides essential information about the mechanics of cutting but the studies on 3-D turning are limited. A 3-D FEA of machining processes is needed to study practical machining operations. This will be very useful for process planners and tool designers to optimize cutting conditions and materials prior to actual production. The force, temperature and stress information provided by the FEA may be used to predict tool wear and according to this information the existing cutting conditions may be altered, if necessary, in order to prolong tool life. The geometry of the cutting tool, workpiece and cutting tool material properties, and tool-chip friction conditions must be defined carefully to obtain reasonable results from finite element .

**Ibrahim A. Al-Zkeri [3]** Used the two-dimensional finite element method (FEM) is used as a tool for understanding the fundamentals of hard turning process and for the prediction of the effect of edge preparation (edge hone radius, chamfer angle) and cutting conditions (cutting speed, feed rate) on the hard turning variables (cutting forces, chip morphology, tool stresses temperature, and residual stresses).The effect of cutting tool edge geometry on several hard turning variables (cutting and thrust forces, chip-tool contact length and shear angle) were predicted using finite element method with reasonable accuracy. The results showed agreement with the trends in measurements. The maximum Von-Mises stress acting on cutting insert with the largest chamfer angle ( $30^{\circ}$ ) has the smallest value (3500 MPa). In addition, the edge with chamfer angle  $20^{\circ}$  causes the biggest stress magnitude (4700 MPa).

**Karpal and Özel et al [4]** had been used 3-D finite element modeling of precision hard turning to investigate the effects of cutting edge micro geometry on tool forces, temperatures and stresses in machining of AISI H13 steel using polycrystalline inserts with two distinct edge preparations. Three components of tool forces and flank wear of the inserts were measured. Inserts with honed micro-geometry cutting edge resulted in lower tool flank wear in all cutting conditions.

**Tugrul O'zel et al [5]** Investigate experimentally the effects of cutting edge geometry, workpiece hardness, feed rate ,cutting speed on surface roughness and resultant forces in the finish hard turning of AISI H13 steel experimentally. Cubic boron nitride inserts with two distinct edge preparations and through hardened AISI H13 steel bars were used. The effects of two-factor interactions of the edge geometry and the workpiece hardness, the edge geometry and the feed rate, and the cutting speed and feed rate are also appeared to be important. Especially, honed edge geometry and lower workpiece surface hardness resulted in better surface roughness. Cutting edge geometry, workpiece hardness and cutting speed are found to be affected on force components. The lower workpiece surface hardness and small edge radius resulted in lower tangential and radial forces.

**Tugrul O'zel [6]** Analysis in his study investigated the influence of edge preparation in cutting tools on process parameters and tool performance by utilizing practical finite element (FE) simulations and high speed orthogonal cutting tests. The predicted process parameters through FE simulations in high speed orthogonal cutting are calculated optimize tool life and surface finish in hard machining of AISI H-13 hot work tool steel. Simulation results provided a distribution of stresses and temperatures at the cutting zone, chip-tool and workpiece-tool interfaces. Numerical simulations include testing different edge preparation geometry for CBN tools at different cutting speeds and feeds. The results showed that the zone of workpiece material formed under the chamfer

acts as an effective rake angle during cutting. The presence of a chamfer affects the cutting forces and temperatures while no significant change in chip formation observed.

## **2-Modelling using the Finite Element Method**

DEFORM-3D software is used to simulate the turning process, which is based on the Lagrangian equation as shown in Fig. 3 . The software is used to simulate the the effects of the edge preparations on temperatures , tool wear , effective strains and stresses in machining of AISI 1045 steel using uncoated carbide inserts .

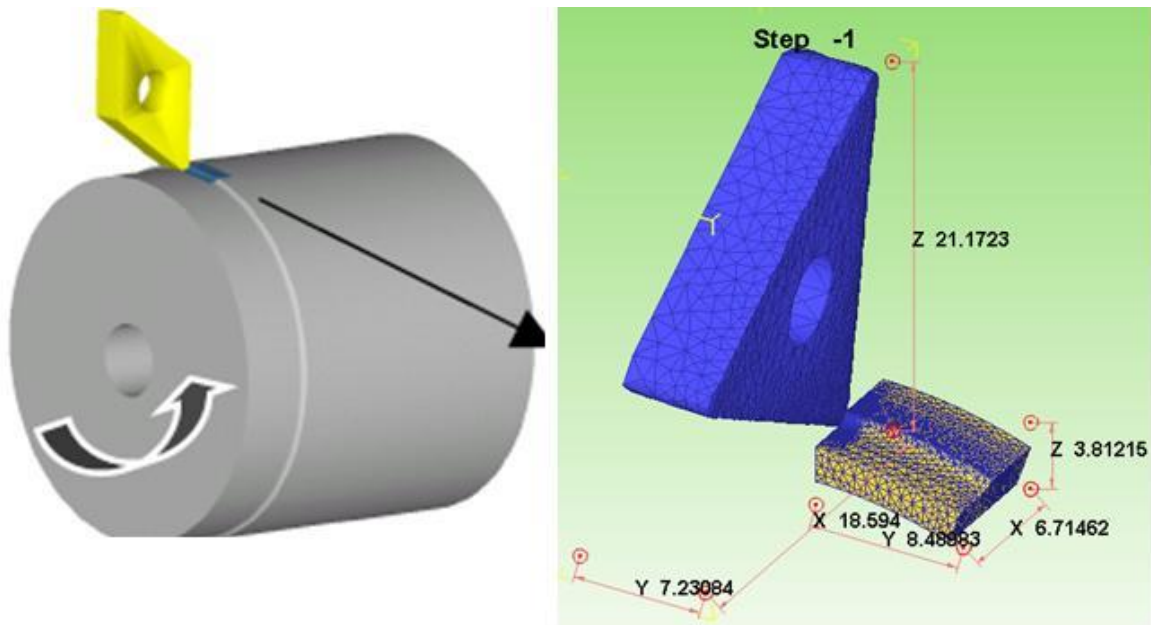


**Figure 3 Finite element simulation of hard turning with uncoated carbide tool**

Currently Deform-3D system has Archard's model and Usui's model apart from the user routine support. Usui's model is used for machining applications to compute insert wear. Archard's model can be used with either isothermal or non-isothermal runs, On the other hand Usui's model can be run only be used with non-isothermal run as it required interface temperature calculations as well [7] and [8] .

Applications of FEM models for machining can be divided into six groups: 1) tool edge design, 2) tool wear, 3) tool coating, 4) chip flow, 5) burr formation and 6) residual stress and surface integrity. The direct experimental approach to study machining processes is expensive and consumes long time.

To solve problem, finite element methods are most frequently used. Modeling tool wear using FEM has advantages over conventional statistical approach because it provides useful information such as deformations, stresses, strain and temperature chip and the work piece, as well as the cutting force, tool wear, tool stress and temperature on the tool working under specific cutting parameter [8].

Usui's equation includes three variables: Sliding velocity between the chip and the cutting tool, tool temperature and normal pressure on tool face. These variables can be predicted by FEM simulation of cutting process or combining analytical method and finite difference method. Therefore Usui's equation is very practical for the implementation of tool wear estimation by using FEM or by using the combination of FDM and analytical method[9].

$$\omega = \int a p v e^{-b/T} dt \text{ -----1}$$

Where  $\omega$ = tool wear  $p$ =interface pressure  $v$ =sliding velocity  $T$ =interface temperature (deg)  $dt$ = time increment  $a, b$  =experimentally calibrated coefficients

The chip formation from initial mesh and tool indentation in the beginning of cutting process until the developed continues chip formations step 50 , 100 ,150 , 200 are as illustrated in figure 4

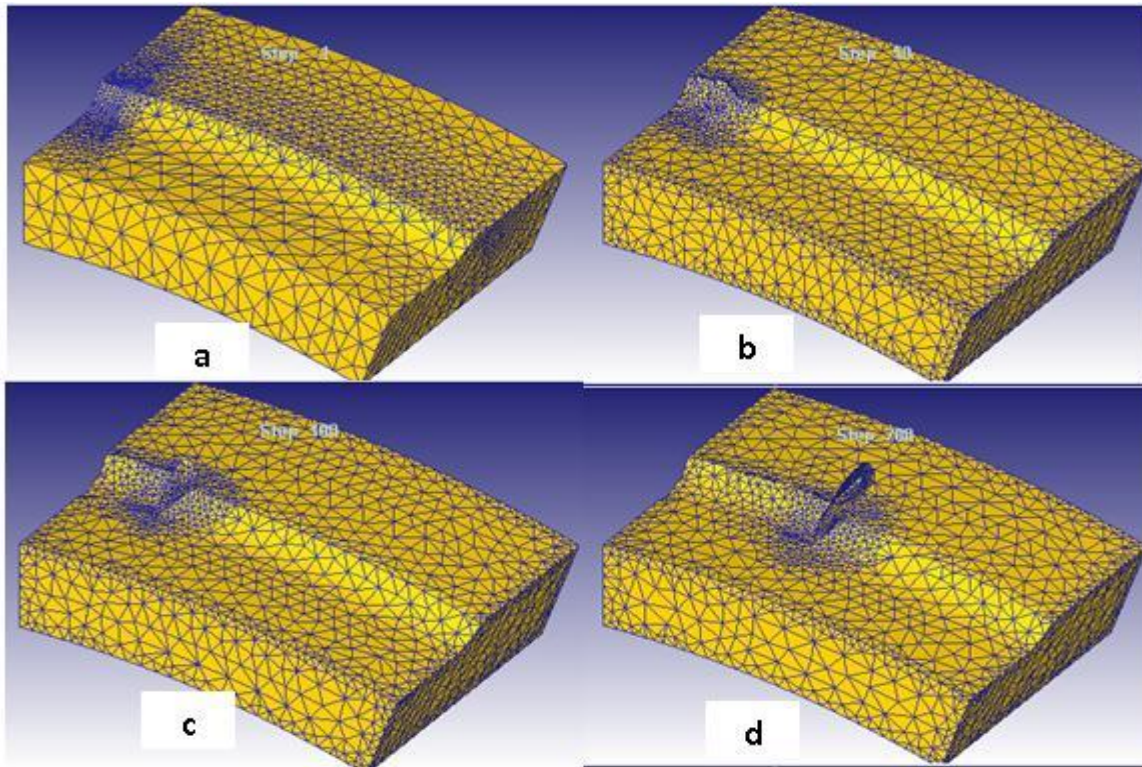


Figure 4 (a) initial mesh (b) chip mesh after 50 step (c) chip mesh after 100 step (d) Developed continues chip at 200 step

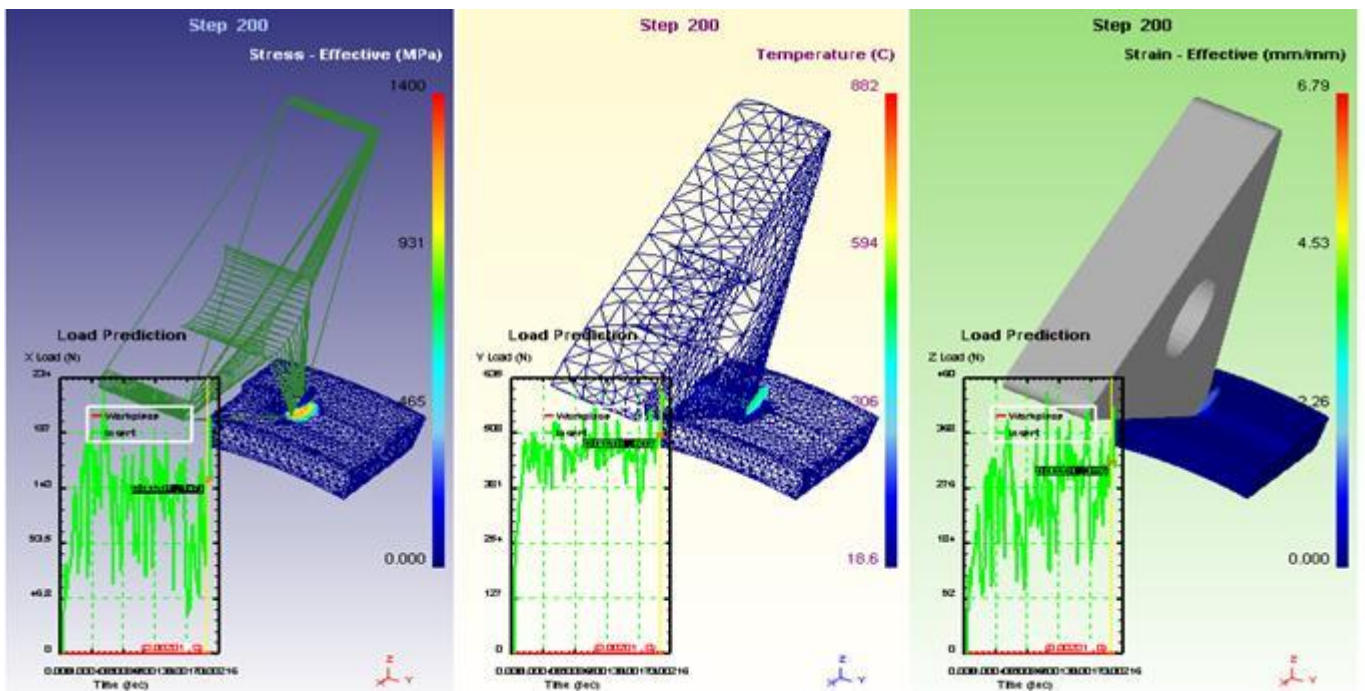


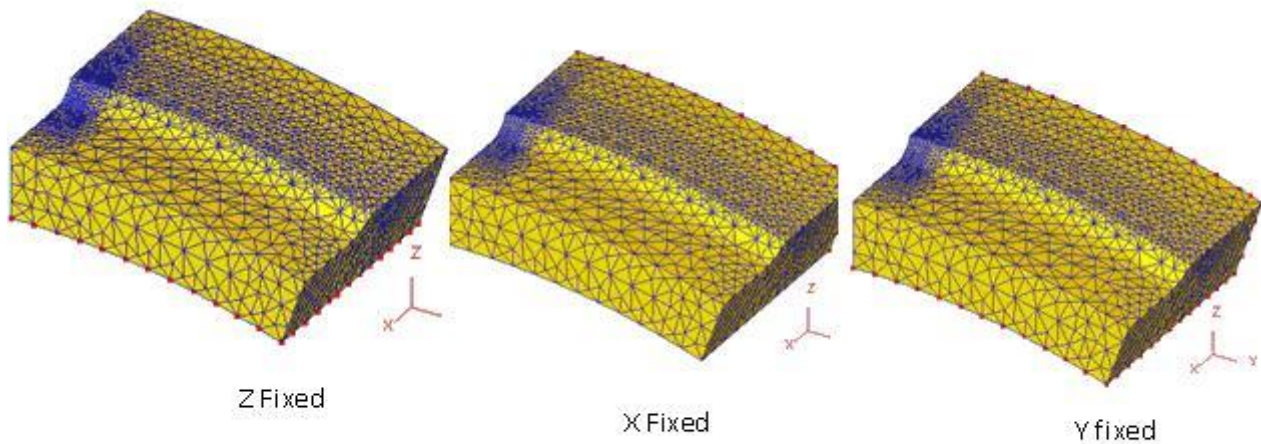
Figure 5 shows an example of transient simulation result for chamfer 0.75mm.

**Table1 cutting condition and tool geometry in the simulation**

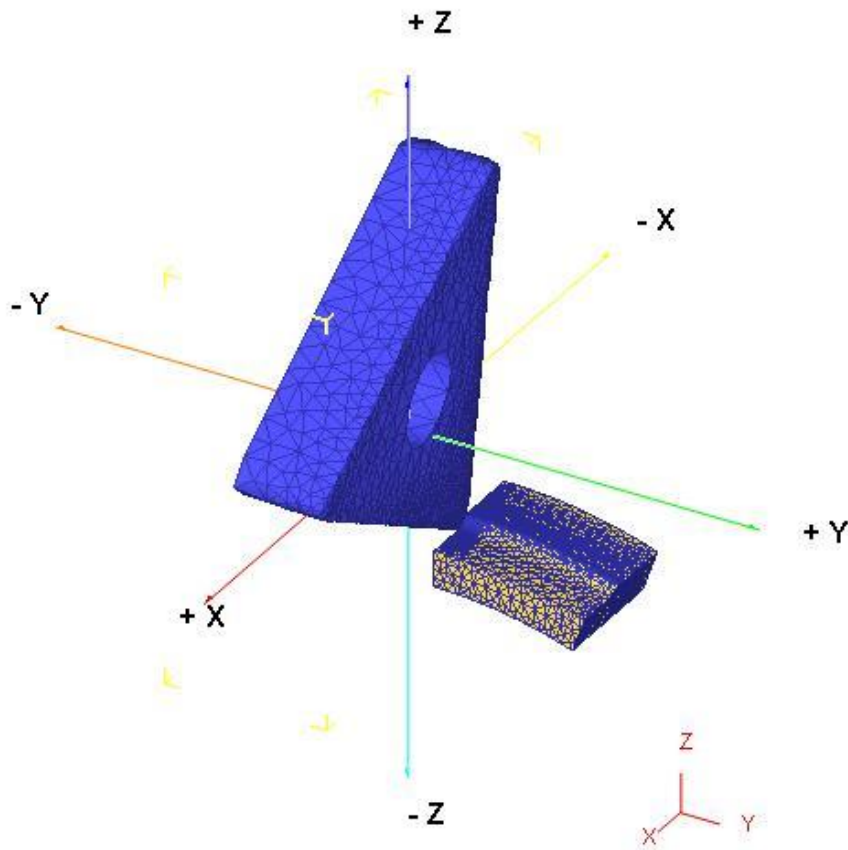
Cutting condition	
Cutting speed	100mm/sec
Feed rate	0.3 mm/rev
Depth of cut	0.5
Tool Geometry of DNMA 432	
Back Rake Angle (BR) (deg)	-5
Side Rake Angle (SR) (deg)	-5
Side Cutting Edge Angle (SCEA)	0
Nose radius mm	0.79375

Table 2 Boundary condition	
Initial Temperature (°C)	20
Shear friction factor	0.6
Heat transfer coefficient at the interface (N/s mm°C)	45

The workpiece and the tool were modeled with 20,000 and 12,000 elements to start with and the adaptive remeshing scheme was implemented to optimize between the computational time and accurate prediction. Referring to fig 6, the base of the workpiece was constrained in all directions. The tool was subjected to move in (+Y) direction at constant speed and constrained against movements in X and Z directions as shown in fig7 . The frictional contacts at the interface between the tool/workpiece and the tool/chip were described by a constant shear hypothesis with the shear factor of 0.6.



**Figure .6 Boundary conditions to Workpiece**



*Figure .7 Boundary conditions to cutting tool (tool move in +Y direction)*

## 2.2 Material property

The properties of the workpiece material (AISI 1045 steel) and insert (tungsten carbide) are shown in table 3,4 5,6 .

*Table 3 Chemical composite of workpiece material 1045*

Metal	C%	Mn%	P%	S%	Si %
Carbon steel 1045	0.43	0.7	0.04	0.5	0.16

*Table 4 Mechanical and thermal properties of workpiece 1045*

Elastic Modulus Gpa	Tensile strength Mpa	Yield Strength Mpa	Hardnes s HB	Elongati on	Poisson ratio
205	585	505	170	12	0.28

*Table 5 Mechanical Properties of tungsten carbide*

Hardness (Knoop)	Modulus of Elasticity (psi)	Compressive strength (Kpsi)	Poisson Ratio
1500	90 x 10 <sup>6</sup>	580	0.24

*Table 6 Thermal Properties of Tungsten Carbide*

Coefficient of Thermal expansion (/ °C)	Thermal conductivity (W/mK)	Heat capacity
56-06	59	15

The workpiece was assumed to be an plastic material. To account for the strain rate and properties, a velocity-modified temperature is calculated using temperature effects on the material the equation:

$$T_{\text{mod}} = T \left[ 1 - v \log \frac{\dot{\epsilon}}{\dot{\epsilon}_0} \right] \text{-----}2$$

where T is the temperature at the point where the properties are to be determined, v the Poisson's ratio, the strain rate, and is the strain rate below which the properties of the material are unaffected by strain rate. Temperatures at the shear plane and tool-chip interface are determined according to the work done in those zones. This is calculated from the shear forces, shear velocities and tool an workpiece material thermal properties using the equations as shown by Oxley equation (1989).

$$\sigma = \sigma_1 \epsilon^n \text{-----}3$$

Where  $\sigma$  and  $\epsilon$  are flow stress and strain,  $\sigma_1$  is the material flow stress at  $\epsilon=1.0$  and n is the strain hardening exponent.  $\sigma_1$  and n depend on velocity modified temperature (Tmod).

In addition to plastic properties of work piece, its thermal properties depending on temperature have to be given to the software for heat transfer calculation. Thermal conductivity, thermal expansion and heat capacity of AISI 1045 are shown in Figure 8,9,10 and 11.

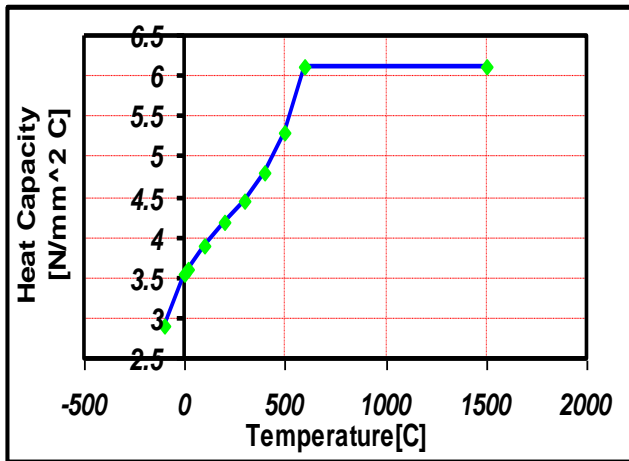


*Figure .8 Heat Capacity of AISI 1045*

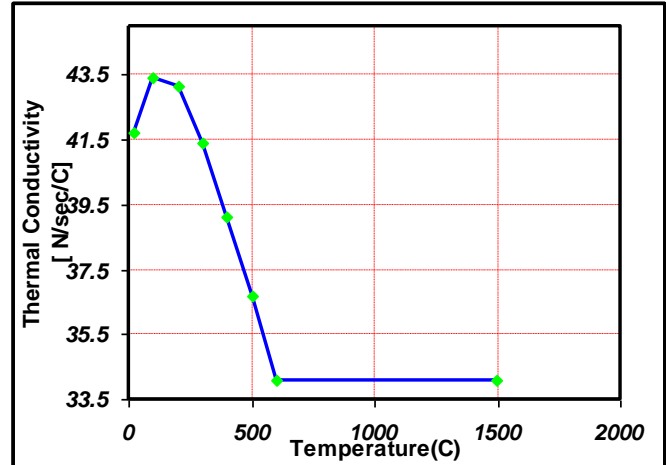


*Figure .9 Thermal Conductivity of AISI 1045*

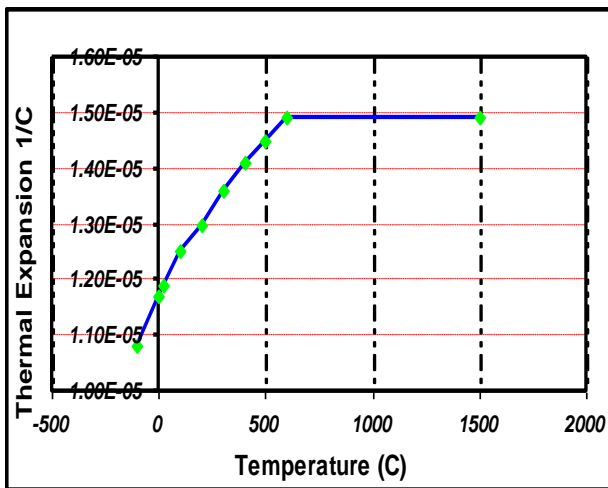


*Figure .10 Thermal Expansion of AISI 1045*

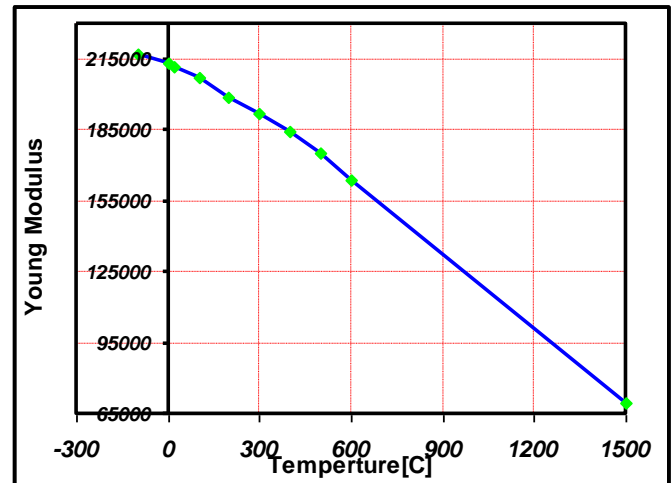


*Figure .11 Young's Modulus of AISI 1045*

### **3-Effect of micro-geometry and corner radius on friction**

Let us reconsider Fig. 3 which demonstrates the 3-D turning with a corner radius tool. Tool chip contact area is redrawn in detail in Fig.12. As can be seen from the figure That the thickness of the chip varies from a maximum value, which is equal to the feed rate, to a minimum value on the tool's corner. Uncut chip thickness is mainly defined by the feed rate and corner radius of the tool. If an edge radius applied to the tip of the cutting tool, cutting efficiency will be low due to small ratio of uncut chip thickness to tool edge radius around that area. Three critical sections A-A, B-B and C-C are indicated in Fig.12. In Section A-A, uncut chip thickness is greater than the edge radius. In Section B-B, the uncut chip thickness becomes equal to the edge radius and rubbing action is more dominant than shearing. In Section C-C the edge radius is larger than the thickness of the uncut chip and the work material is rubbed against the workpiece. This rubbing action will result in increased strains and heat generation on the tool-workpiece interface.



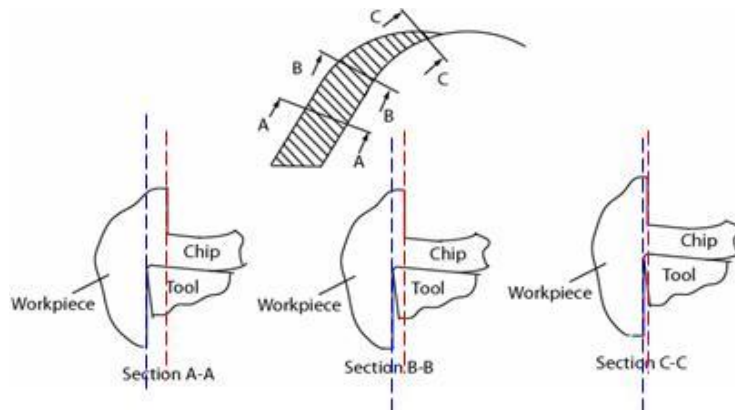


**Figure .12 Relationship between edge preparation and uncut chip thickness along corners radius .**

Since chip load varies along the tool corner radius, friction at tool-chip interface should also vary and needs to be determined carefully. The determination of a varying friction in 3-D analysis is left as a future work. The detailed interaction of the cutting tool and workpiece is explained in Figure 13. It can be seen that chip load is a function of depth of cut, feed rate and tool corner radius. In this figure, it is important to observe that the thickness of the chip, which is shown as the hatched area, varies along tool corner radius.

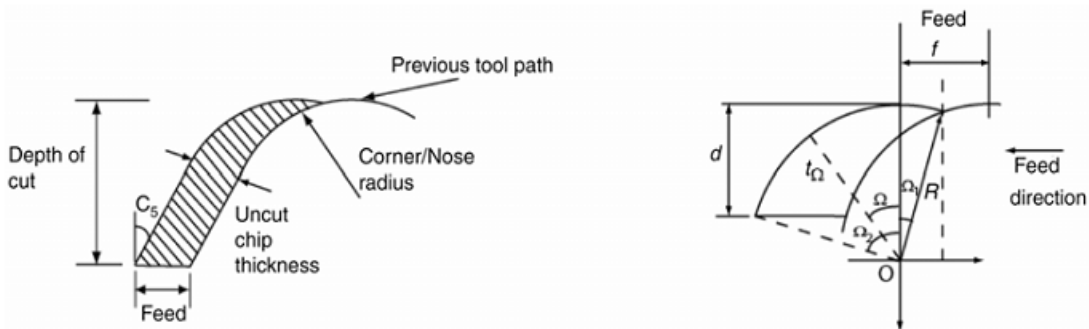


**Fig 13. Chip load in typical turning operation with a corner radius tool**

$$\Omega_1 = -\sin^{-1}\left[\frac{f}{2R}\right]$$

$$\Omega_2 = \cos^{-1}\left[\frac{R-d}{R}\right]$$

$$t_\Omega = R + f \sin \Omega - \sqrt{R^2 - f^2 \cos^2 \Omega}$$

$$t_\Omega = R - \frac{R-d}{\cos \Omega}$$

Where :  $\Omega$  sweep angle

when  $\Omega \leq \tan^{-1}\left[\frac{R \sin \Omega_2 - f}{R-d}\right]$  -----4

when  $\Omega > \tan^{-1}\left[\frac{R \sin \Omega_2 - f}{R-d}\right]$

## **4- Results and Discussion**

Table 3 Shows the Simulations result for various combinations of edge preparations, the value of wear depth and cutting force after running time 0.002sec (3.4mm).

### **4-1-Effect of edge preparation on work piece and cutting tool temperature .**

As shown figure 14. The chip temperature obtained from the simulation process is between  $604\text{ C}^0$  to  $804\text{ C}^0$ . The minimum temperature is achieved at the chip which is machined by edge for chamfer tool (0.075mm).

As shown figure 15. The cutting tool temperature on rake face obtained from the simulation process is between  $90.4\text{ C}^0$  to  $128\text{ C}^0$ . The minimum temperature is achieved at the edge of honed (0.75)mm. Temperature field in the workpiece, chip and the tool were also calculated in 3-D FEA. A representative temperature field in workpiece and the chip is given in Fig16. Temperature fields around the edge for honed tool are given in Fig.17. The "hot spot" is found at the honed face 90.4 ,99.8 , 106 for 0.75 , 0.5 , 0.25 mm (honed radius).The generated temperature on the chip, machined surface and tool edge can be seen in Figure 18 ,19 .that the most of heat or generated temperature is carried away by the chip (about 70%), there was maximum of generated temperature on shear zone about  $627\text{ C}^0$  and only around  $90.4\text{ C}^0$  generated on the tool (around 10%) and the rest remain absorbed by work piece

These were agreeable with [10], where by assuming that all the cutting energy was converted to heat, so a considerable amount of heat was generated at the following three distinct zones; **1)** Shear zone (75%); **2).**Chip sliding on the tool face (20%), and **3).** Tool sliding on the workpiece machined surface (5%) which was neglected for perfectly sharp cutting tools. These are shown in Fig 20.

The temperature on work piece surface is necessary to considered, because based on the detailed microstructure analysis shows that worn out tools can cause over heated of the machined surface and change the microstructure of the work material. That change can increase the hardness of the work material's machined surface to become very hard and brittle, so the information on work piece are very useful to avoid such increase in hardness as explained [9].

### **4-2- The effect of edge preparations on the cutting forces**

In the finish hard turning , cutting force was found the largest among the force components as shown in fig 21. Furthermore ,cutting force is found to be greater in land tool (0.3)mm compared to honed tool(0.75)mm . These are agreeable with [5].

### **4-3-Analysis of stress and shear on chip and work piece**

Effective stress distribution was also calculated through post-analysis where the cutting tool is defined as elastic body. Resultant stress distribution is shown for chamfered tool in Fig 22. shows that the highest stress and strain were found on the primary deformation zone, which resulted the stress of about 1240 MPa and strain about 2.18 mm/mm in fig 23.

These are agreeable with the theory denoted that the maximum heat produced is at shear zone because there is the highest plastic deformation of the metal in this primary shear zone. The major deformation during cutting process were concentrated in two region close to the cutting tool edge, and the bigger deformation was occurred in the primary deformation zone, followed by secondary deformation zone; sliding region and sticking region as described by [11] and [12].

All of simulation results for every edge preparation combination setting were plotted as shown in Figure 24. show that maximum value effective stress reach at chamfer 0.5 while the minimum value at honed (0.75mm).

#### **4-4-The effect of edge preparation on tool flank wear .**

Figures 25 ,26 ,27 , show the simulation of depth of wear after running 200 steps. After step 53, the cutting force begin to stable or just get a bit fluctuation on (465.6 N) in fig 24 . Figure 28 shows the wear depth at the nose of carbide cutting edge for honed (0.075) edge the during machining. The wear depth is 0.00935mm. The maximum wear depth for edge preparation land (0.2) is 0.0181mm.

All of simulation results for every side cutting edge angle combination setting were plotted as shown in Figure 29. shows that the minimum wear depth reach at honed edge , This phenomenon is agreeable with experiment done by [4].

#### **5-CONCLUSIONS**

The effect the edge preparation is to increase the strength of the cutting edge by providing more gradual transition between the clearance edge and the rake face of the tool. For simulation results, the following conclusions can be drawn:

- 1-Hone micro-geometry inserts have tendency to result in lower forces, hence lower tool wear.
- 2-Chamfer micro-geometry provides higher localized stress concentration.
- 3-The highest stress and strain on workpiece occurred in the primary shear zone due to the highest deformation in this region, followed by the secondary shear zone. The maximum generated temperature was also found on shearing zone.

#### **Reference**

- 1-Ibrahim A. Al-Zkeri, ."*Finite Element Modeling Of Hard Turing*" , Doctor Dissertation , The Ohio State University,2007
- 2- Mikell P.Groover , "*Fundamentals Of Modern Manufacturing Material ,Processes and System ,Second Edition*" , John Wiley and Sons.Inc. 2007
- 3- W. Grzesik, M. Bartoszuk and P. Niesłony "*Finite Element Modelling Of Temperature Distribution In The Cutting Zone In Turning Processes With Differently Coated Tools*" . 13<sup>Th</sup> International Scientific Conference On Achievement In Mechanical and Material Engineering ,Poland
- 4-Yiğit Karpat and Tuğrul Özel , "*3-D FEA Of Hard Turning: Investigation Of PCBN Cutting Tool Micro- Geometry Effects*". Department Of Industrial and Systems Engineering Rutgers University Piscataway, New Jersey , Transactions Of NAMRI/SME ,Volume 35 ,2007
- 5-Tugrul OZel · Tsu-Kong Hsu · Erol Zeren , "*Effects Of Cutting Edge Geometry, Workpiece Hardness, Feed Rate and Cutting Speed On Surface Roughness and Forces In Finish Turning Of Hardened AISI H13 Steel*", International Journal Advance Manufacturing Technology (2005) 25: 262–269
- 6 -Tugrul OZel , "*Modeling Of Hard Part Machining: Effect Of Insert Edge Preparation In CBN Cutting Tools*" , Journal Of Materials Processing Technology 141 (2003) 284–293
- 7-Deformtm-3D, 2007. "*Deform-3d Tool Wear Lab*", Scientific Forming Technologies Corporation. El-Hofy, [www.Deform-3d.Com](http://www.Deform-3d.Com)
- 8- Mackerle, J., , "*Finite Element Analysis and Simulation of Machining:*" *Journal of Materials Processing Technology*, Vol. 86,1999, pp. 17–44.
- 9-Jaharah, A.G., Choudhury.A., Masjuki. H. H., Che Hassan. C.H., 2009. "*Surface Interguity Of AISI H13 Tool Steel In End Milling Process*", International Journal Of Mechanical and Materials Engineering (IJMME), Vol. 4 (2009), No. 1, Pp. 88 -92.
- 10-Amit Gupta, "*Thermal Modeling and Analysis Of Carbide Tool Using Finite Element Method*" ,Thesis , Mechanical Engineering Department Thapar Institute Of Engineering and Technology , Deemed University , June 2005 , India .

- 11- Kalthori. V ." *Modelling and Simulation Of Mechanical Cutting*", Doctoral Thesis, Institutionen For Maskinteknik, Sweden , 2001
- 12-Hendri Yanda, Jaharah A.Ghani, Che Hassan Che Haron "*The Effect Rake and Clearance Angle On The Wear Carbide Cutting Tool*", *Engineering E-Transaction (Issn 1823-6379) Vol. 4, No. 1, June 2009, Pp 7-13*
- 13- Deform-3D ,2005 ,Manual , Documentation For 3D- Machining Wizard ,"*Machining Template-3D*" SFTC, [www.Deform-3d.Com](http://www.Deform-3d.Com)

**Table 3. Cutting condition to the simulation models and material properties**

Edge Preparation	Tool flank wear	Effective Stress W.P Mpa	Chip Temperature C <sup>0</sup>	Effective Strain	Cutting Forces N	Tool Temperature C <sup>0</sup>	Effective Stress Tool Mpa
<b>Chamfer 0.025</b>	0.0147	1200	652	1.91	456.2	98.1	1600
<b>Chamfer 0.05</b>	0.0126	1240	683	2.18	488.2	120	3480
<b>Chamfer 0.075</b>	0.0148	1220	604	2.19	465.6	101	1570
<b>Land 0.05</b>	0.0147	1230	688	2.07	578.6	91.5	1510
<b>Land 0.1</b>	0.0138	1220	691	2.55	531.4	92.9	1310
<b>Land 0.2</b>	0.0181	1230	810	3.83	550.8	128	2280
<b>Land 0.3</b>	0.0143	1220	804	3.87	609	96.9	1200
<b>Honed 0.25</b>	0.0132	1230	657	2.94	519.4	99.8	1440
<b>Honed 0.5</b>	0.0147	1200	682	2.10	481	106	1590
<b>Honed 0.75</b>	0.00935	1200	627	1.89	461.6	90.4	1490
<b>Sharp</b>	0.0129	1220	673	1.98	572.2	100	1670

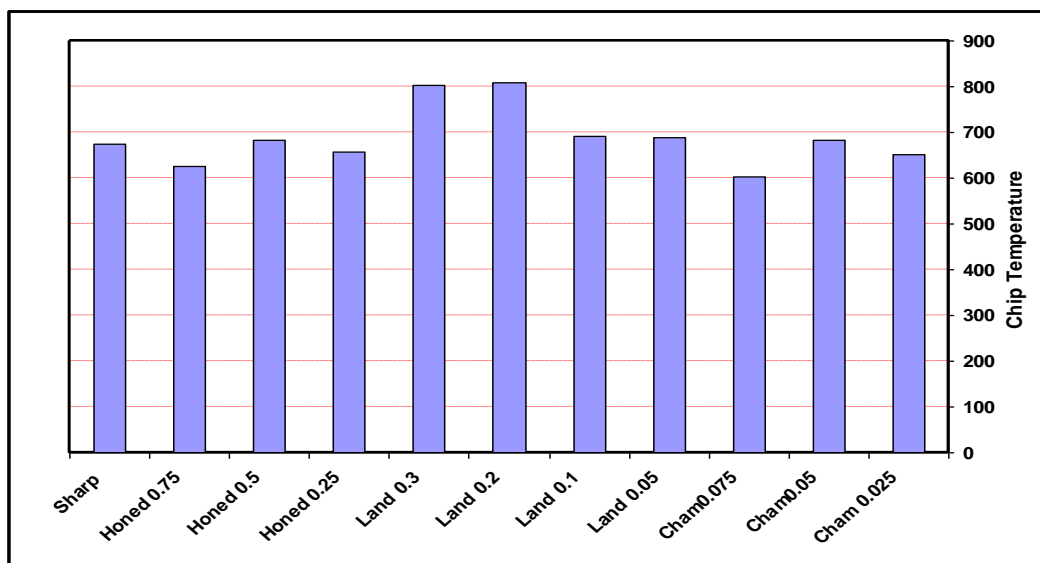


**Figure 14. The Effect of edge preparation on chip temperature**

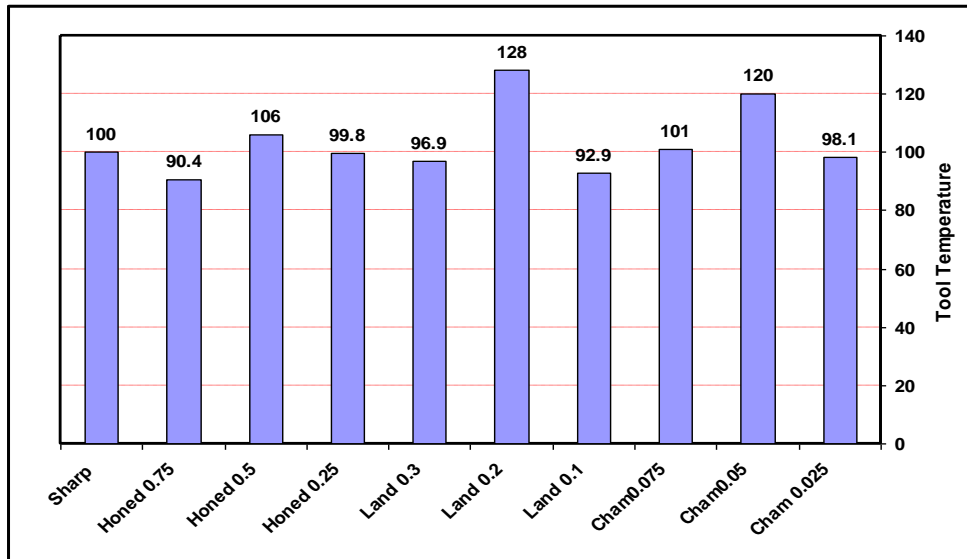


*Figure15. The Effect of edge preparation on tool temperature*

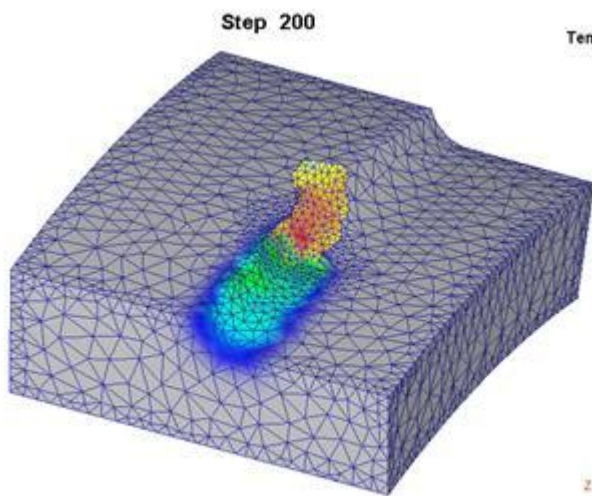


*Figure 16. Predicted temperature fields in the chip honed edge(0.75mm)*

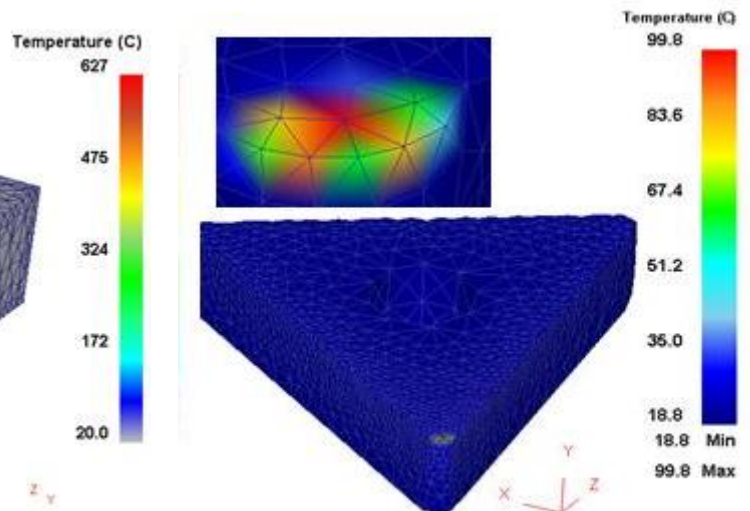


*Figure17. Temperature fields in honed*

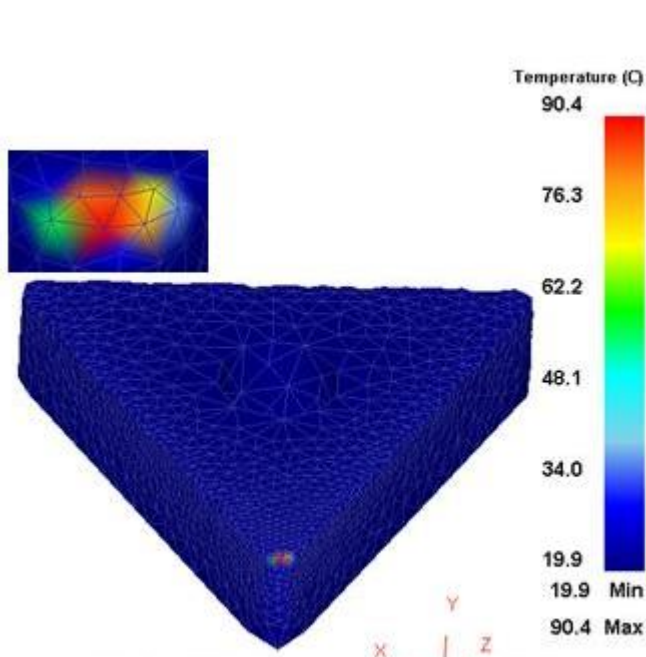


*Figure18. Temperature fields in honed*

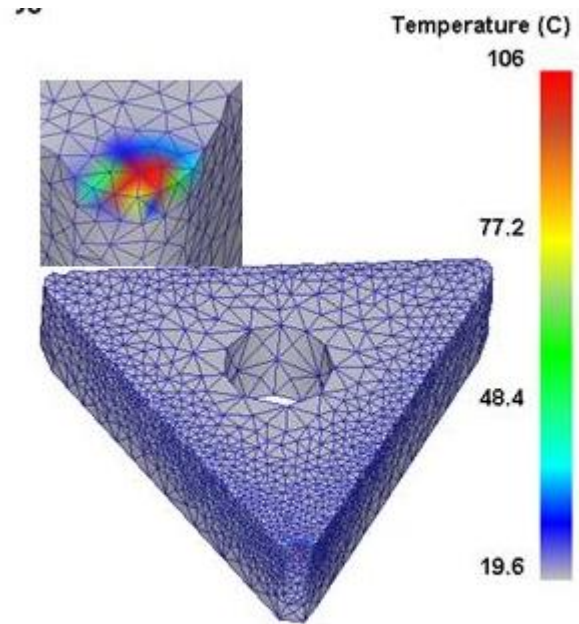


*Figure 19. Temperature fields in honed*

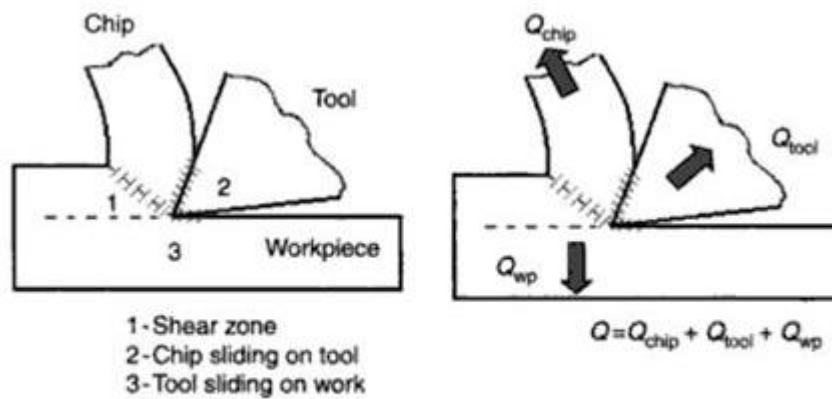


*Figure20. Heat generated and heat dissipation in metal cutting (Source: El-Hofy, 2008)*

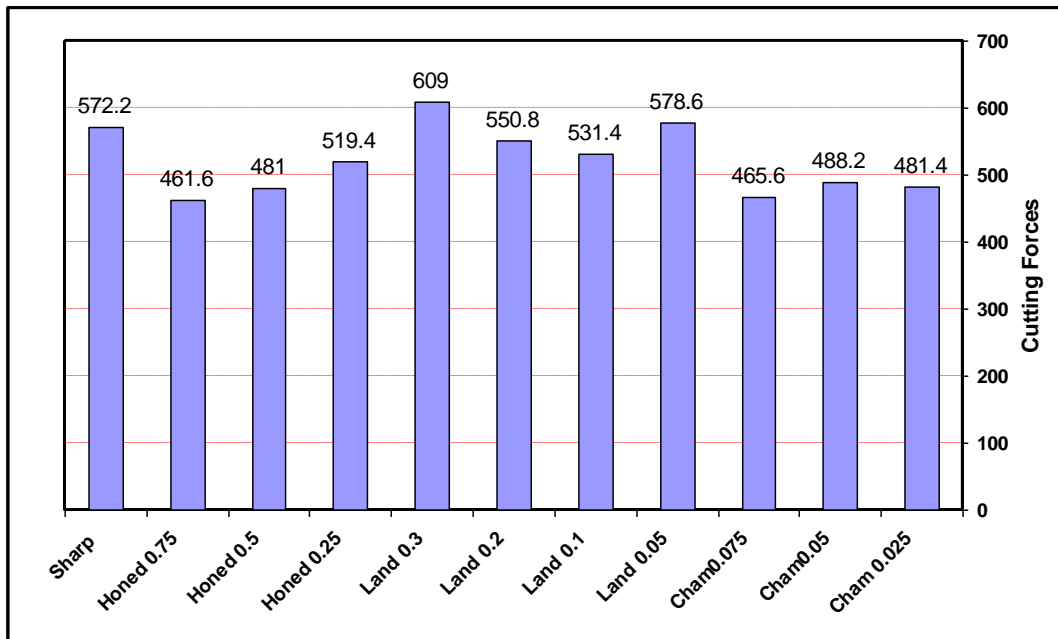


*Figure 21. The Effect of edge preparation on the cutting forces*

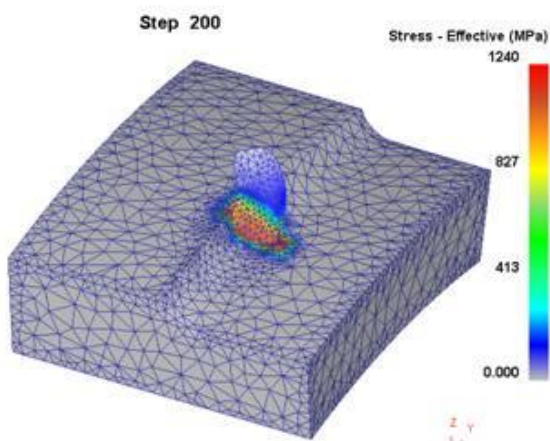


*Figure 22 Effective strain distribution on chamfer (0.05mm)*

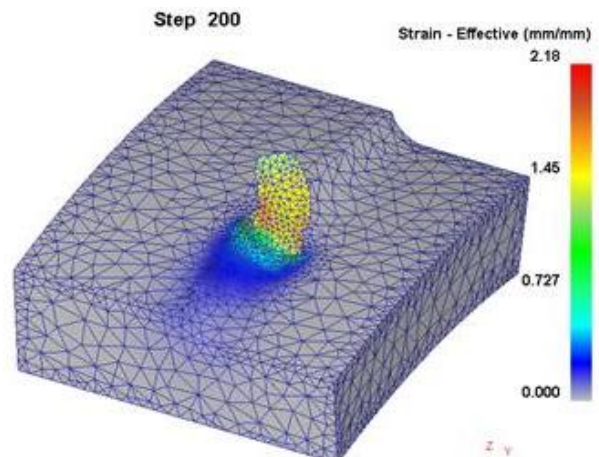


*Figure 23. Effective strain distribution on chamfer (0.05mm)*

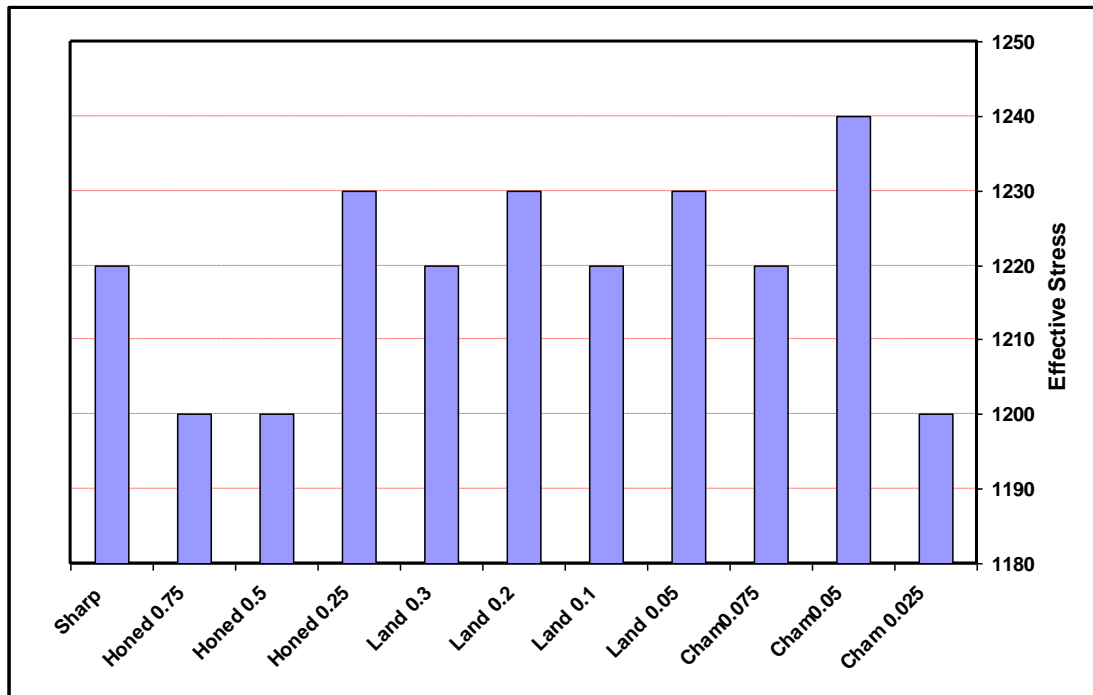


*Figure 24. Effective edge preparations on the effective stress*

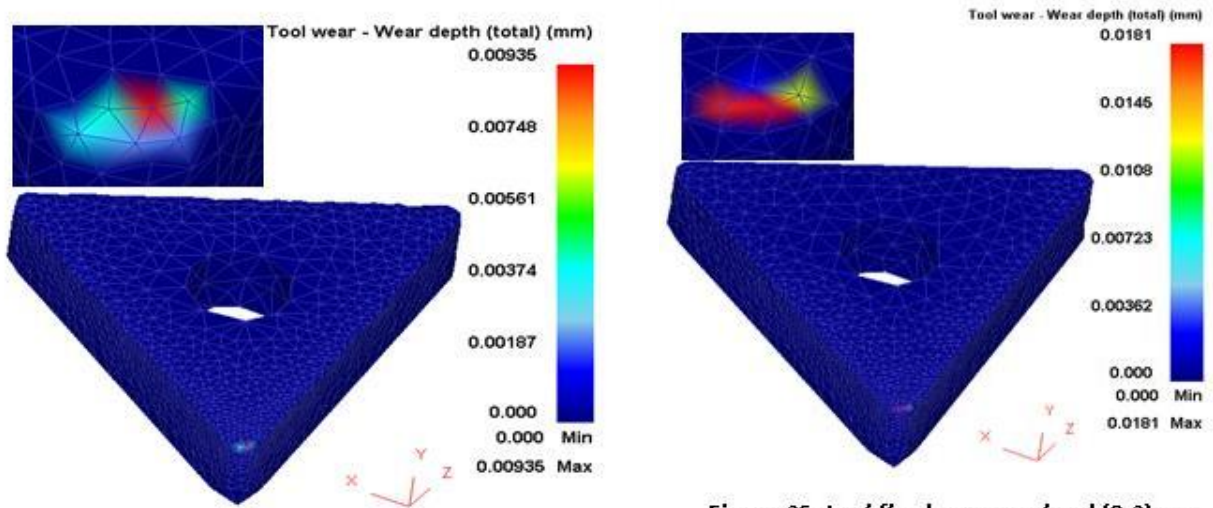


*Figure 25. tool flank wear on honed (0.75)mm*

*Figure 26. tool flank wear on land (0.2)mm*



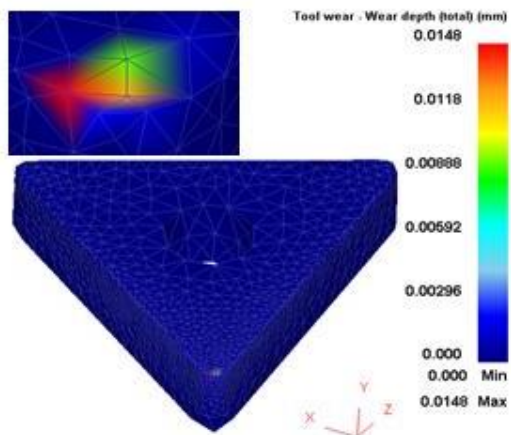


**Figure 27. tool flank wear on Chamfer**

**(0.075)mm**

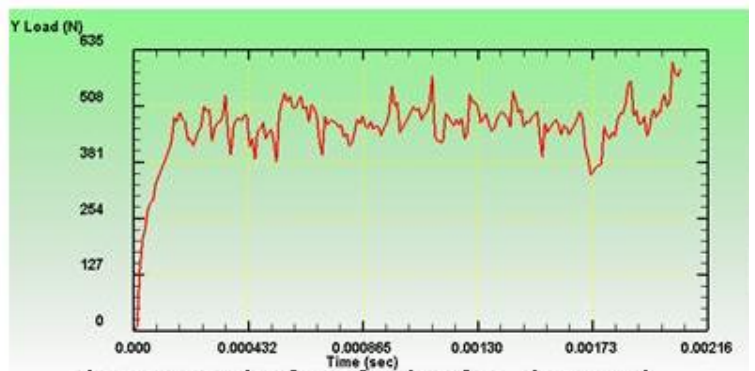


**Figure 28 . cutting force for chamfer (0.075mm)**

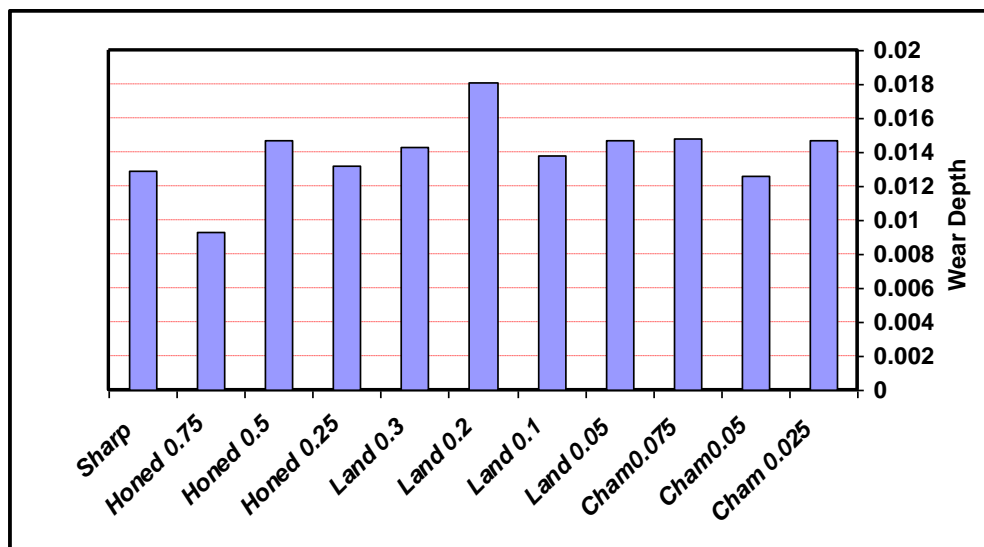


**Figure 29. Effect of edge preparation on tool flank wear**